DIPOLE MODEL ANALYSIS OF HERA DATA WITHIN THE HERAFitter FRAMEWORK*

A. Łuszczak

Institute of Physics, Tadeusz Kościuszko Cracow University of Technology
Podchorążych 1, 30-084 Kraków, Poland
agnieszka.luszczak@ifj.edu.pl

(Received May 8, 2013)

We analyse the precise DIS reduced cross section data from HERA using the BGK dipole model with valence quarks. We show that it is possible to describe the HERA data very well using solely the dipole model gluon density with added valence quarks from the usual pdf's.

DOI:10.5506/APhysPolB.44.1537
PACS numbers: 12.38.Bx, 13.60.Hb

1. Introduction

The saturation model of Golec-Biernat and Wüsthoff (GBW) [1] has been very successful in describing both the inclusive, F_2, and diffractive, $F_2^{D(3)}$, structure functions of proton at low values of the Bjorken variable x. The model was then improved by Bartles, Golec-Biernat and Kowalski (BGK) [2] by including the DGLAP evolution of the gluon density, whose effects are important for the small-r part of the dipole cross section. This allowed to describe the new, more precise, HERA data. However, this model does not take into account valence quarks, which are added in the measured F_2 data from HERA. That is why we added the valence quarks from the usual pdfs, to be more consistent with the HERA data. It is the novelty of this analysis, which was done within HERAFitter framework [3–5]. HERAFitter Package is a ready platform to analyse new data and their impact.

The main motivation for this study is provided by the observation that in the usual pdfs approach the gluon density is not very well defined since the F_2 measurements are not very sensitive to its contribution. The gluon density contributes to F_2 mainly through the evolution of the sea quarks, the

* Presented at the Cracow Epiphany Conference on the Physics After the First Phase of the LHC, Kraków, Poland, January 7–9, 2013.

direct contribution is only of the order of a few percent. This is different than in the case of $F_{\rm L}$, which in the collinear factorization approach, is mainly determined by the gluon density. In the case of F_2, the uncertainties due to higher order QCD effects are of the order of 10%, whereas for $F_{\rm L}$ they are much larger, of the order of 100%. This indicates that gluon density is not very well defined within the usual pdf scheme. On the other hand, in the dipole models, the gluon density is directly connected to the sea quarks and, therefore, also to F_2. This interpretation is confirmed by the successful predictions for $F_{\rm L}$ obtained from the F_2 measurements analysed within the dipole models.

The different role of the gluon density in the two approaches could show a way to improve the understanding of the physical properties of the gluon density.

2. Dipole models

In the dipole picture, the deep inelastic scattering is viewed as a two-stage process; first, the virtual photon fluctuates into a dipole, which consists of a quark–antiquark pair (or a $q\bar{q}g\ldots$ system) and in the second stage, the dipole interacts with the proton [6]. This proccess is shown in Fig. 1. Here, r is dipole size and z is longitudinal momentum fraction of the quark/antiquark. We can factorise this process as dipole formation and dipole interaction

$$\sigma^{\gamma p} = \frac{4\pi^2\alpha_{em}}{Q^2} F_2 = \sum_f \int d^2r \int_0^1 dz \, \left|\Psi^\gamma\left(r,z,Q^2,m_f\right)\right|^2 \hat{\sigma}(r,x)\,. \qquad (1)$$

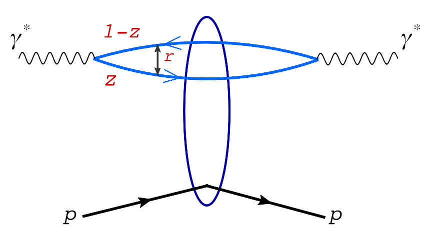

Fig. 1. The photon–proton interaction in the dipole formalism at small x.

Dipole–proton interaction is written as

$$\hat{\sigma}(r,x) = \sigma_0\left(1-\exp\left\{-\hat{r}^2\right\}\right)\,, \qquad \hat{r} = r/R_s(x)\,. \qquad (2)$$

Dipole denotes a quasi-stable quantum mechanical state, which has a very long life time $\propto 1/m_p x$ and a size r which remains unchanged during scattering. The scattering amplitude is a product of the virtual photon wave function with the dipole cross section. The photon wave function describes the probability to find a dipole within a virtual photon and the dipole cross section determines a probability of the dipole–proton scattering.

Several dipole models have been developed to describe various DIS reactions. They vary due to different assumption made about the behavior of dipole cross sections. In the HERAFitter three representative models are implemented:

— the original (GBW) [1] dipole saturation model,

— the colour glass condensate approach to the high parton density regime (IIM) [7],

— a modified GBW model which takes into account the effects of DGLAP evolution (BGK) [2].

2.1. GBW model

In the GBW model, the dipole–proton cross section σ_{dip} is given by

$$\sigma_{\mathrm{dip}}\left(x,r^2\right)=\sigma_0\left(1-\exp\left[-\frac{r^2}{4R_0^2(x)}\right]\right), \tag{3}$$

where r corresponds to the transverse separation between the quark and the antiquark, and R_0^2 is an x dependent scale parameter which has a meaning of saturation radius, $R_0^2(x)=(x/x_0)^{\lambda}$. The free fitted parameters are the cross-section normalisation σ_0 as well as x_0 and λ.

2.2. IIM model

The IIM (Iancu, Itakura, and Munier) model assumes an improved expression for dipole cross section which is based on the Balitsky–Kovchegov equation [8]. The explicit formula for σ_{dip} can be found in [7]. The free fitted parameters are the alternative scale parameter $\tilde{R}$, x_0 and λ.

2.3. BGK model

The BGK model modifies the GBW model by taking into account the DGLAP evolution of the gluon density. The dipole cross section is given by

$$\sigma_{\mathrm{dip}}\left(x,r^2\right)=\sigma_0\left(1-\exp\left[-\frac{\pi^2r^2\alpha_{\mathrm{s}}\left(\mu^2\right)xg\left(x,\mu^2\right)}{3\sigma_0}\right]\right). \tag{4}$$

The evolution scale μ^2 has the form $\mu^2 = C_{\mathrm{BGK}}/r^2 + \mu_0^2$. In this model the gluon density, which is parametrized at some starting scale μ_0^2 by

$$xg\left(x, \mu_0^2\right) = A_g x^{-\lambda_g} (1-x)^{C_g} \tag{5}$$

is evolved to larger scales, μ^2, using LO or NLO DGLAP evolution. The free fitted parameters for this model are σ_0, μ_0^2 and 3 parameters for gluon A_g, λ_g, C_g. The fit results were found to be independent of the parameter C_{BGK}, which was, therefore, fixed as $C_{\mathrm{BGK}} = 4\ \mathrm{GeV}^2$, in agreement with the original BGK fits.

3. Dipole model with valence quarks

The dipole models are valid in the low-x region only. In this region, the valence quark contribution is small and, therefore, was usually neglected. This was justified as long as the experimental errors were relatively large. The new HERA F_2 data have a precision better than 2% so since the contribution of valence quarks is of the order of 5% it is no more justified to neglect it. A straightforward solution of this problem is to take the valence quark contribution from the standard pdfs fits and just add it to the dipole predictions. In this approach, the dipole contribution plays the role of the sea quarks in the standard pdfs. This procedure is justified by the fact that the sea quark contribution disappears at larger x. The HERAfitter program is well suited for this approach since the dipole model and the valence quarks contributions are a part of the same framework.

4. Results from fits with the BGK model

The BGK model is best suited for investigation of the interplay of the dipole and valence quarks contributions because it uses the DGLAP evolution, which is known to provide the best description of the HERA data, see Table I.

TABLE I

Dipole model BGK fit without valence quarks for σ_r for H1ZEUS-NC-$(e+p)$ and H1ZEUS-NC-$(e-p)$ data in the range of $Q^2 \geq 3.5$ and $Q^2 \geq 8.5$, and $x \leq 0.01$.

No.	Q^2		σ_0	A_g	λ_g	C_g	C_{BGK}	μ_0^2	Np	χ^2/Np
1	$Q^2 \geq 3.5$	NLO	40.4	1.6	-0.249	12.3	1.6	0.4	197	1.10
2	$Q^2 \geq 8.5$	NLO	32.5	1.7	-0.256	11.7	1.5	0.2	156	0.80

Indeed, the fits with the BGK dipole model alone show a very good agreement with data, the χ^2 values are similar to the χ^2 values of the standard pdfs fits shown in Table II.

TABLE II

HERAPDF fit with valence quarks for σ_r for H1ZEUS-NC-$(e+p)$, H1ZEUS-NC-$(e-p)$ data in the range $Q^2 \geq 3.5$ and $Q^2 \geq 8.5$, and $x \leq 0.01$. χ^2 is calculated in the region $x \leq 0.01$.

No.	Q^2	HF Scheme	Np	χ^2	χ^2/Np
1	$Q^2 \geq 3.5$	RT	197	220.64	1.12
2	$Q^2 \geq 3.5$	ACOT Full	197	206.85	1.05
3	$Q^2 \geq 8.5$	RT	156	131.04	0.84
4	$Q^2 \geq 8.5$	ACOT Full	156	131.04	0.84

In Table III, we show four fits of the BGK dipole model with valence quarks in the LO and NLO approach. We have five fitted parameters: σ_0, A_g, λ_g, C_g, μ_0^2. Alternative values of the parameter cBGK fixed as 4.0 were also investigated: 1.5, 2.0, 6.0, 8.0, 10.0, 12.0. In these fits, we set the non-zero quark mass because it allows for a better description of the current data. We also fix the minimal value μ_0^2 of the scale μ^2 to 1 GeV^2 for the gluon evolution. Since the parameters σ_0, and λ_g are strongly correlated, we have performed a systematic search of the best χ^2. The fit results are very good.

TABLE III

Dipole model BGK fit with valence quarks for σ_r for H1ZEUS-NC-$(e+p)$ and H1ZEUS-NC-$(e-p)$ data [9] in the range $Q^2 \geq 3.5$ and $Q^2 \geq 8.5$, and $x \leq 0.01$. The calculation was done in ACOT Full HF Scheme.

No.	Q^2		σ_0	A_g	λ_g	C_g	C_{BGK}	μ_0^2	Np	χ^2/Np
1	$Q^2 \geq 3.5$	LO	66.6	4.0	-0.039	18.6	4.0	5.3	196	0.930
2	$Q^2 \geq 8.5$	LO	63.6	4.2	-0.036	19.8	4.0	5.1	157	0.790
3	$Q^2 \geq 3.5$	NLO	79.4	3.2	-0.021	13.7	4.0	6.7	196	0.927
4	$Q^2 \geq 8.5$	NLO	67.5	1.9	-0.14	15.9	4.0	3.8	157	0.781

The quality of the fits of the BGK dipole model with valence quarks matches the quality of HERAPDF fits in the low x region.

5. Comparison with HERA data

In Fig. 2, we show the comparison of the BGK dipole model predictions with the combined H1 and ZEUS collaborations data [9] on the reduced cross section

$$\sigma_{\mathrm{r}}^D = F_2^D - y^2 F_{\mathrm{L}}^D / \left(1 + (1-y)^2\right) . \tag{6}$$

We included in the structure function the charm contribution. The solid lines correspond to the results of the NLO BGK dipole model fit number 3 from Table III. We found good agreement with data from HERA.

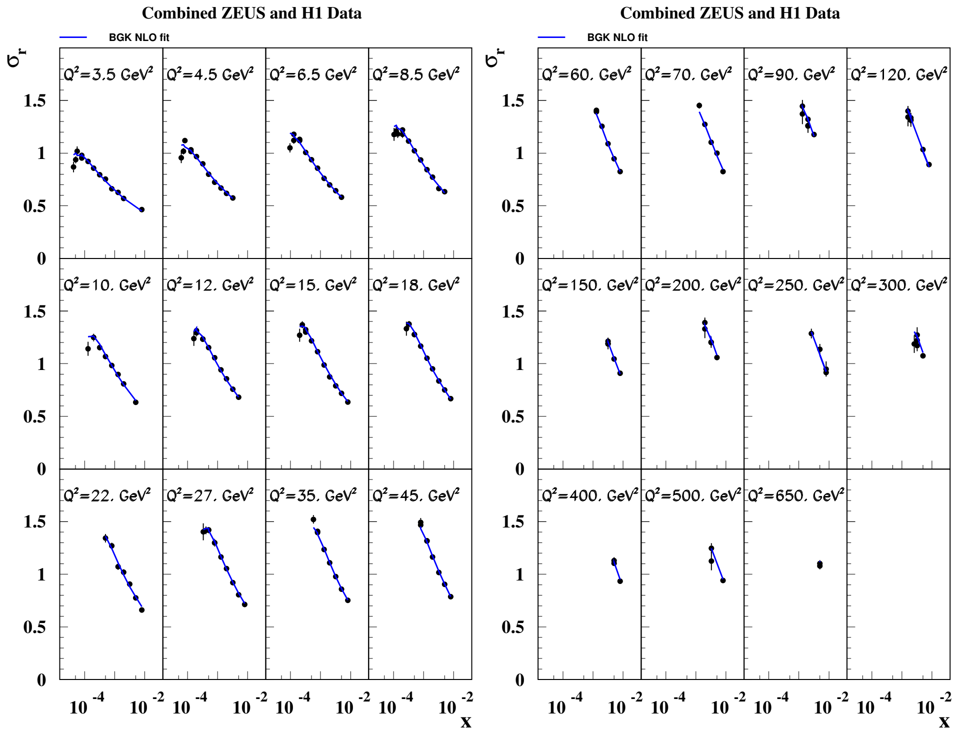

Fig. 2. Comparison of the NLO dipole fit from Table III with HERA data.

6. Prediction for $F_{\rm L}$ function

In this section, we show prediction for the $F_{\rm L}$ proton structure function measured at the given values of Q^2 and x. The present measurement of $F_{\rm L}$ function [9] supersedes the published H1 result [10] in the common region of phase space. The $F_{\rm L}$ data presented here extend down to Q^2 of 1.5 GeV^2, which is much smaller than the minimum Q^2 value of previously published results by H1 [10] and ZEUS [11]. Consequently, $F_{\rm L}$ is measured down to $x \approx 0.00003$ for the first time. We show prediction from BGK dipole model for $F_{\rm L}$ proton structure function in LO and NLO approach. The predictions describe data very well.

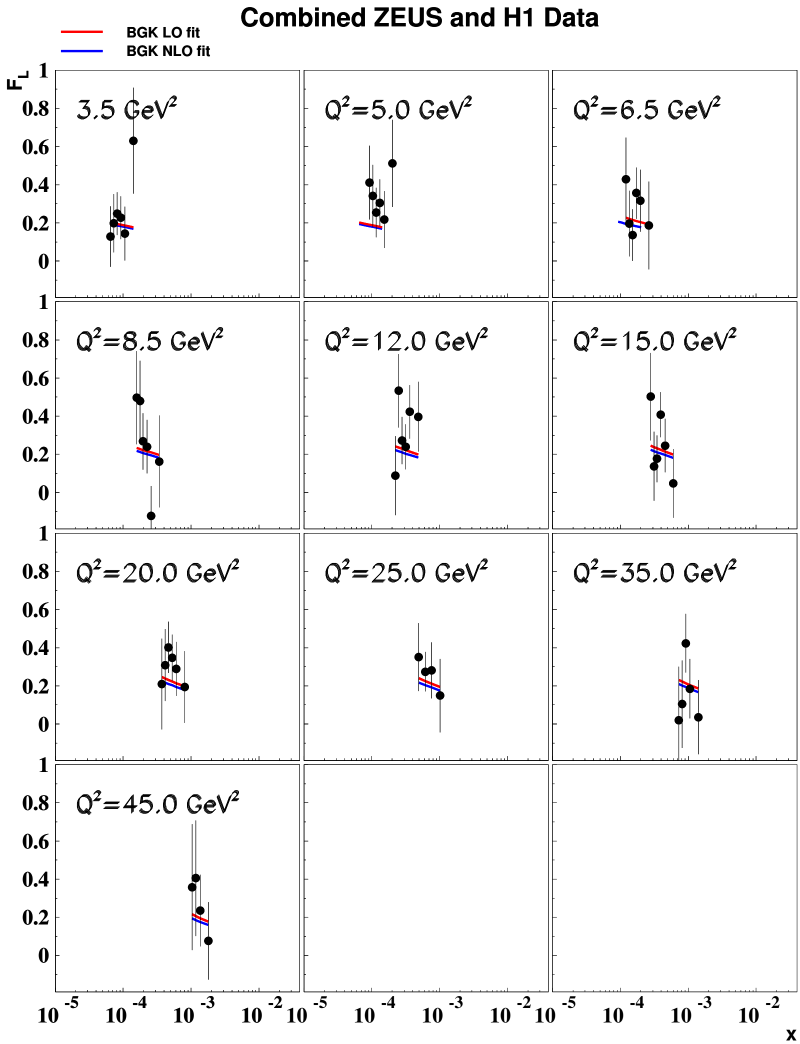

Fig. 3. F_{L} of the fit number 4 from Table III.

7. Summary

We have shown that it is possible to simply add the contribution of the valence quarks obtained in the standard pdfs fits to the BGK dipole contribution and obtain excellent fit results. In presented analysis, we use BGK dipole model, which has very similar physics interpretation as pdfs, *i.e.* DGLAP evolution in the k_{t} factorization scheme (in contrast to the collinear factorization for pdfs). The quality of the fits from the BGK dipole model with valence quarks and without valence quarks are very good. This could show a way to improve the pdfs fits because the gluon density within dipole model is less sensitive to the higher order corrections than in the collinear factorization scheme, which is usually used.

I would like to express my gratitude to Henri Kowalski and Sasha Glazov from DESY with whom this work has been done.

REFERENCES

[1] K. Golec-Biernat, M. Wüsthoff, *Phys. Rev.* **D59**, 014017 (1999).
[2] J. Bartels, K. Golec-Biernat, H. Kowalski, *Phys. Rev.* **D66**, 014001 (2002).
[3] F.D. Aaron *et al.* [H1 Collaboration], *Eur. Phys. J.* **C64**, 561 (2009).
[4] M. Botje, *Comput. Phys. Commun.* **C182**, 490 (2011).
[5] F.D. Aaron *et al.* [H1 and ZEUS collaborations], *J. High Energy Phys.* **1001**, 109 (2010).
[6] N.N. Nikolaev, B.G. Zakharov, *Z. Phys.* **C49**, 607 (1991).
[7] E. Iancu, K. Itakura, S. Munier, *Phys. Lett.* **B590**, 199 (2004).
[8] I. Balitsky, *Nucl. Phys.* **B463**, 99 (1996).
[9] H1 Collaboration, *Eur. Phys. J.* **C71**, 1769 (2011).
[10] F.D. Aaron *et al.* [H1 Collaboration], *Phys. Lett.* **B665**, 139 (2008).
[11] F. Chekanov *et al.* [ZEUS Collaboration], *Phys. Lett.* **B682**, 8 (2009).